Surface saturation control on the formation of wurtzite polytypes in zinc blende SiC nanofilms grown on Si-(100) substrates*

Liu Xing-Fang(刘兴昉)†, Sun Guo-Sheng(孙国胜), Liu Bin(刘 斌), Yan Guo-Guo(闫果果), Guan Min(关 敏), Zhang Yang(张 杨), Zhang Feng(张 峰), Dong Lin(董 林), Zheng Liu(郑 柳), Liu Sheng-Bei(刘胜北), Tian Li-Xin(田丽欣), Wang Lei(王 雷), Zhao Wan-Shun(赵万顺), and Zeng Yi-Ping(曾一平)

Key Laboratory of Semiconductor Materials Science, Institute of Semiconductors, Chinese Academy of Sciences, Beijing 100083, *China*

(Received 30 December 2012; revised manuscript received 7 March 2013)

We investigate the formations of wurtzite (WZ) SiC nano polytypes in zinc blende (ZB) SiC nanofilms hetero-grown on Si-(100) substrates via low pressure chemical vapor deposition (LPCVD) by adjusting the Si/C ratio of the introduced precursors. Through SEM, TEM, and Raman characterizations, we find that the nanofilms consist of discrete WZ SiC nano polytypes and ZB SiC polytypes composed of WZ polytypes (WZ + ZB) and disordered ZB SiC polytypes, respectively, according to Si/C ratios of 0.5, 1.5, and 3. We attribute the WZ polytype formation to being due to a kinetic mechanism based on the Si/C surface saturation control.

Keywords: SiC, wurtzite, zinc blende, nanofilm

PACS: 68.55.–a, 71.20.Nr, 81.07.Bc, 81.15.Kk **DOI:** 10.1088/1674-1056/22/8/086802

1. Introduction

As a wide bandgap semiconductor, SiC exhibits excellent physical and chemical properties such as high electron saturation velocity, high breakdown field, high thermal conductivity and being chemically inert.[1,2] These features make SiC an advanced semiconductor material for electronic applications in fields of high power, high temperature, and harsh environments.[3] On the other hand, SiC is assumed to have more than 250 polytypes divided into zinc blende (ZB), wurtzite (WZ), and rhombohedron (RH) groups. WZ polytype such as 4H–SiC has a wider bandgap than ZB polytype such as 3C–SiC, which makes WZ polytypes more suitable for high power electronics than ZB polytypes.[4]

WZ polytypes are thought to be unfavourable thermodynamic stable phases at a temperature lower than 1500 K, while ZB polytypes are the most thermodynamic stable phases in common sense.[5] To date, WZ SiC films can be homoepitaxially grown on commercial available wafers at a temperature higher than 1630 K,[6,7] while ZB SiC films can be relatively easily heteroepitaxially grown on Si wafers in a wide range from 1250 K to 1600 K.[8] ZB monocrystalline hetero-growth on Si substrate has been deeply investigated for decades.[9–12] Various studies have been carried out to improve the monocrystalline quality,[9] reduce the growth temperature,[10,11] and increase the wafer sizes.[12] In these respects considerable progress has been achieved. However, WZ monocrystalline polytypes have been reported only on substrates with the same hexagonal polytype structures, such as 4H–SiC,[13–15] 6H–SiC[16] or sapphire wafers.[17] So far , the growth of WZ polytypes on substrates with ZB polymorphy is difficult and WZ monocrystalline growth has not been reported yet.

In this work, we report on the growth of WZ SiC nano polytypes on Si-(100) substrates using low pressure chemical vapor deposition (LPCVD). Simply by varying the Si/C ratio of the precursors, we can obtain discrete WZ SiC nano polytypes or ZB SiC polytype composed of WZ polytypes. We propose a kinetic mechanism based on the Si/C surface saturation controlling[18] to explain our results of WZ polytypes formation on Si-(100) substrates. The results may pave the way for future WZ SiC heteroepitaxial growth and WZ SiC based applications.

2. Experimental procedure

The SiC nanofilms were grown on n-type Si-(100) substrates by LPCVD at 1400 K under an H_2 ambience of 5.33×10^3 Pa. The silicon and the carbon precursor were SiH_4 and C_2H_4, respectively,[19] and dopant precursor was not used in this study. Firstly, the substrates were carefully treated with surface contamination cleaned by an RCA processing and native oxides removed by a 30% diluted HF solution bathe for 30 s. Then the substrates were loaded into the LPCVD chamber with a base pressure of 1.3 Pa. Before the films growth, the substrates were subject to heat treatments at 1300 K under an H_2 ambience of 9.33×10^3 Pa for 1 h. The precursors were introduced into growth chamber for SiC nanofilm growth, when the chamber pressure decreased to 5.33×10^3 Pa and the temperature increased to 1400 K.

*Project supported by the National Natural Science Foundation of China (Grant No. 61274007) and the Beijing Natural Science Foundation, China (Grant No. 4132074).

†Corresponding author. E-mail: liuxf@mail.semi.ac.cn

© 2013 Chinese Physical Society and IOP Publishing Ltd

For three typical growth processing environments, the gas flows of SiH_4/C_2H_4 were set to be 2 sccm/2 sccm, 3 sccm/1 sccm, and 6 sccm/1 sccm, which made Si/C ratios of 0.5, 1.5, and 3, respectively. The high pure H_2 as carrier gas was fixed at 3 slm during the whole growth processing. The growth time is about 10 min∼20 min.

The surface morphology and structure of each sample were characterized by a Hitachi S-4800 field-emission SEM (FESEM) operated at 15 kV. The cross-sectional structures were characterized by TEM investigations, which were carried out using a Tecnai G2 F20 U-TWIN operated at 200 kV. Raman scattering measurements were performed in a backscattering geometry by a Jobin-Yvon HR 800 instrument with a solid-state laser source of 632.8-nm wavelength in a macroscopic configuration.

3. Results and discussion

Figure 1 shows FESEM images of three types of nanofilms on different scales. As shown in Fig. 1(a), it is found that discrete SiC grains with an Si/C ratio of 0.5, show the prism shapes, and have an in-plane orientation preference on the substrate surface. Since SiC grains are distributed discretely, the substrate surface can be observed through spacers among these individual SiC crystallites. We notice that there are prim pits like inverted quadrangular frustum pyramids on the substrate. These pits are caused by gas etching (reducing gas) at high temperatures. These etch pits are about 1 μm∼2 μm in lateral size, and smaller pits are not observed even in a magnified SEM image (Fig. 1(b)). The WZ polymorphy of this nanofilm will be identified by Raman spectra in Fig. 3. When the Si/C ratio increases to 3, the compact nanocrystallites make up the SiC nanofilm, which covers the whole substrate surface (Fig. 1(c)). This morphology is often observed in polycrystalline ZB SiC heteroepitaxially grown on silicon substrates.[20] As shown in Fig. 1(d), basically, the nanofilms consist of regular arranged SiC nanopillars with an Si/C ratio of 1.5 and in-plane grain sizes of about 100 nm–200 nm, and they are different from other nanofilms shown in Figs. 1(a) and 1(c).

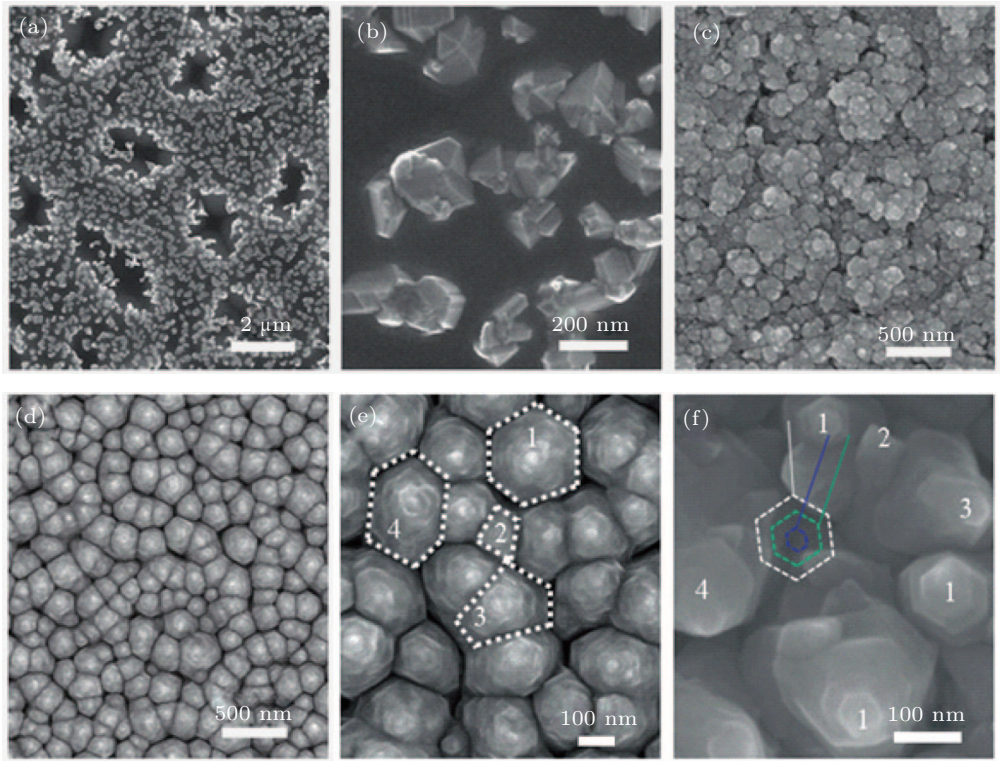


Fig. 1. (color online) SEM morphologies of three types of nano films. (a) WZ SiC nano polytype. (b) Magnified image of panel (a). (c) ZB SiC nano polytype. (d) WZ + ZB SiC nano polytype for growth time of 20 min, and (f) that for 10 min. (e) Magnified image of panel (d).

In addition, sidewall facets are thought to be evidence for the emergence of ZB or/and WZ structures. Figure 1(e) shows the top views of nanopillars of ZB, WZ, and their mixtures. For a perfect WZ structure nanopillar (labelled as 1, denoted as P1 for short, unless otherwise stated), just like a short segment of a nanowire,[21] it usually appears in six outmost sidewall facets. These facets can be indexed as families, and they are approximately equal in length since the na-

ture of surfaces is nonpolar.[21] For a ZB structure nanopillar P2 (labelled as 2), it has four outmost sidewall facets. When ZB structure is mixed with WZ structures, the out-of-plane appearance of these nanopillars loses either ZB shape or WZ shape, and the outmost sidewall facets are no longer equal in length. The nanopillar P3 has five outmost sidewall facets and the nanopillar P4 has two longer sidewall facets other than the other four ones. The number of outmost sidewall facets probably depends on the radial growth of WZ polytype in growth frontier and the proportion of WZ in ZB structure. If the outmost sidewall facets of individual crystallite grow in an unconstrained style, the crystallite will grow up to be a six-sidewall facet nanopillar (P1) or a four-sidewall facet nanopillar (P2). If not, other nanopillars will appear, such as the five-sidewall facet nanopillar (P3), the prolonged six-sidewall facet nanopillar (P4), or distorted nanopillars (around P1). The axial growth is different from the radial growth. The topmost parts of the nanopillars lose WZ/ZB polytypes characteristics, and are composed of random nanofacets which make them look like domes (P1∼P4). Nevertheless, mesas with characteristic sidewall facets are still observed in each individual nano pillar, and can be seen more clearly in early growth stage. As growth time decreasing, except P2, which is a ZB nanopillar and has no mesa, nanopillars, such as P1, P3, and P4, have obvious mesa structures. P1 (Fig. 1(f)) has six sidewall facets, and mesas with proportional sizes come into being in different growth stages (three dotted hexagons represent the three topmost mesas). It should also be noticed that the topmost mesa of each individual nanopillar is flat in its early growth stage (Fig. 1(f)) and grows up into dome finally (Fig. 1(e)). This is probably due to the difference in the growth kinetics of each facet among the several topmost mesas.[22]

Figure 2(a) shows the cross-sectional TEM image near the interface between the WZ + ZB SiC nanofilm and the silicon substrate. The interface is very smooth, which indicates good epitaxial growth of SiC on the Si substrate. Moreover, stacking faults bundles (SFBs) are observed in the deposited SiC nanofilm. This can be further confirmed by the SAED pattern (Fig. 2(b)). The SAED exhibits spotty strips. The diffraction spots in strips can be identified as WZ SiC (hexagonal polytype) diffraction spots and ZB SiC ones.[23,24] Indeed, there are basically ZB SiC structures with obvious WZ structures in the high resolution TEM image (Fig. 2(a)), which is different from other work where either strip-like or inclusion WZ structures can be observed.[25,26] We know that the ZB and the WZ structures follow ABCABC and ABABAB stacking sequences, respectively, where each letter represents an Si–C bilayer at a different relative position. Supposing that the initial SiC structure is a ZB structure (ABCABC), when stacking faults occurring, several Si–C bilayers are misplaced, thereby creating locally a WZ structure (ABABAB). Misplaced alternate stacks at the radial growth frontier may be responsible for the WZ shapes (Figs. 1(d)–1(f)).

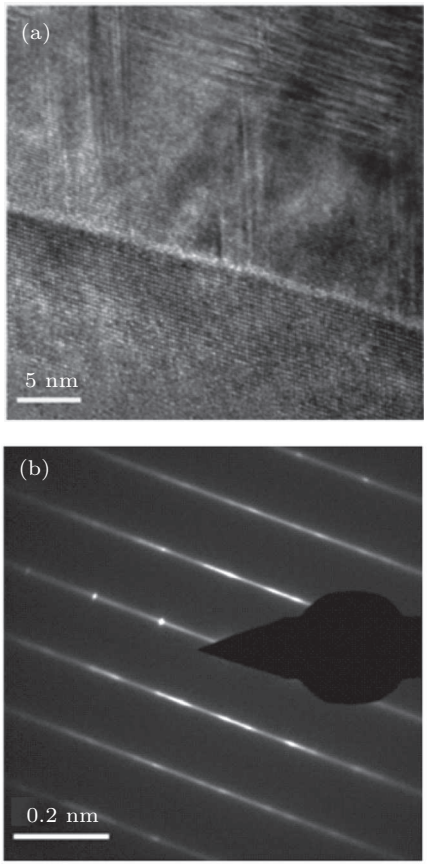


Fig. 2. (a) TEM image near the interface between the WZ + ZB SiC nano film and the silicon substrate. (b) The corresponding SAED pattern, which shows six-fold symmetry and strip-like pattern, representing crystalline WZ structure and SFBs in this region.

Figure 3 shows Raman spectra of the obtained SiC nanofilms in a range of 600 cm^{-1}–1100 cm^{-1}. In a backscattering geometry, four modes of FTA, FTO, FLA, and FLO are visible.[27] As an Si/C ratio of 0.5, one weak Raman FLA peak can be identified as FLA(4/4) located at $\sim$ 610 cm^{-1}. No FTO peak appears at FTO section, and the second order TO modes of silicon occur at FLO section in a range of 940 cm^{-1}–970 cm^{-1},[28] which is folding SiC fingerprint identification if there appears any SiC Raman peak in this FLO section. It is reasonable for the obtained Raman peak information since the deposited film consists of discrete SiC crystallites and silicon directly exposed to Raman ray. Thus, the FLA mode is the only clue for judging from Raman peaks that the SiC nanofilm is composed of WZ polytype (4H). When the Si/C ratio reaches 3, one broad FTO(0) peak located at $\sim$ 793 cm^{-1} and one weak FLO(0) peak at $\sim$ 970 cm^{-1} can be identified as TO mode and LO mode of ZB SiC polytype (cubic SiC). Compared with the standard TO mode and LO mode of monocrystalline cubic SiC, the counterparts of the obtained SiC have red shifts of 3 cm^{-1} and 2 cm^{-1}, respectively. It indicates that the obtained nanofilm is not fully

relaxed and is under tensile stress since $\Delta\omega_{TO} < 0$, according to $\omega_{TO}(cm^{-1}) = (795.9 \pm 0.1) - (1125 \pm 20)\Delta a_{\parallel}/a_0$,[29] where ω_{TO} is the TO frequency under stress, $\Delta\omega_{TO}$ the Raman shift, $\Delta a_{\parallel}/a_0$ the in-plane strain, and a_0 the equilibrium lattice constant. This result is in common sense of tensile stress in the ZB SiC film hetero-grown on silicon substrates since the lattice mismatch between ZB SiC and silicon is $\sim 20\%$ ($a_{SiC} = 0.43$ nm and $a_{Si} = 0.538$ nm) and the thermal expansion mismatch is $\sim 8\%$.[30]

As an Si/C ratio of 1.5, there are two separate Raman peaks at the FTO section (Fig. 3(b)). The main peak located at 795 cm^{-1} can be identified as FTO(0) peak of the ZB SiC polytype, and the next peak at 765 cm^{-1} can be identified as WZ FTO(1). No FTO peak is observed at FTO section, and a strong peak located at 965 cm^{-1} can be identified as the FLO(0) peak of the WZ SiC polytype. We notice that the ZB FTO(0) peak is asymmetrical on the low-frequency side. This is probably due to the presence of a WZ polytype (6H) folded in the main peak.[30] The deposited WZ + ZB mixed nanofilm is also under tensile stress since $\Delta\omega_{TO} = -1\ cm^{-1} < 0$, which is one third of the tensile stress for the ZB nanofilm. This indicates that the mixed WZ polytypes release tensile stress to a certain extent.

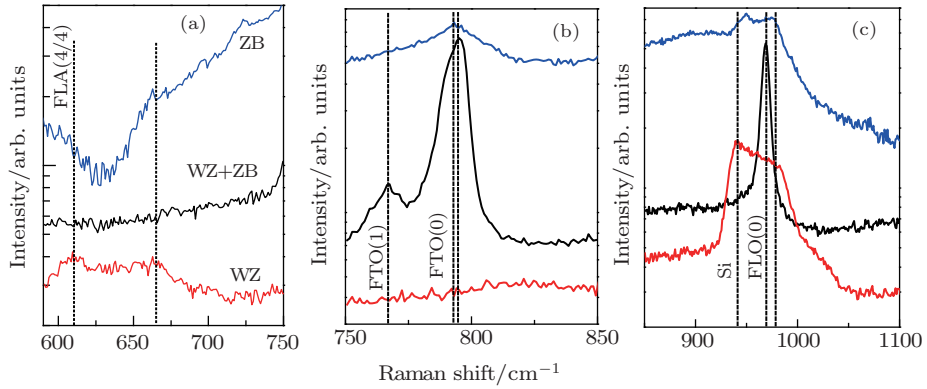


Fig. 3. (color online) Raman spectra of the obtained SiC nano films in (a) FLA section, (b) FTO section, and (c) FLO section. The FLA peak of WZ polytype (4H) is shown in panel (a); the FTO peaks and the FLO peaks of ZB polytype (3C), and WZ + ZB polytypes are shown in panels (b) and (c).

Finally, we explain the mechanism of the WZ polytypes formation in the ZB nanofilms. It has been reported that the ratio of Si/C is regarded as one of the key points for the formation of WZ SiC polytypes at relatively low temperatures. Besides, the partial pressure of the Si source (or the C source) in the forming gases also plays an important role. These two factors result in the supersaturation change in the film deposition zone, which determines the Gibbs free energy of WZ/ZB polytypes formation.[31] The formation of ZB polytype is favored under Si rich conditions when high vapor partial pressure and high supersaturation of Si are provided. On the contrary, if C rich with low supersaturation in the deposition zone is provided, the formation of WZ polytype is favored. The opinion that the WZ/ZB polytypes generation is primarily determined by the C vacancy concentration in the deposition zone has also been proposed by Lebedev *et al.*[26] In our work, when an Si/C ratio of 0.5 is provided, which supplies excess C in the deposited zone, the deposited nanofilm is composed of WZ SiC polytypes. When the Si/C ratio increases to 3, which is high enough to form high carbon vacancy concentration, the ZB SiC polytype nanofilm is deposited. The WZ + ZB SiC polytype nanofilm is obtained at an Si/C ratio of 1.5, which is probably because of the intermediate conditions when Si is rich but with low supersaturation.

4. Conclusions

In summary, we have obtained SiC nanofilms composed of wurtzite (WZ) polytypes and/or zinc blende polytype (ZB) hetero-grown on Si-(100) substrates via LPCVD by adjusting the ratio of Si/C of introduced precursors. When the Si/C ratios are 0.5 and 3, the deposited SiC nanofilms consist of discrete WZ nano polytypes and disordered ZB SiC polytypes, respectively. The most outstanding point is that nanofilms with ZB SiC polytypes composed of WZ polytypes have also been obtained under a growth condition of an Si/C ratio of 1.5. This is deduced from a comprehensive analyses of sidewall facets SEM morphologies, cross-sectional high resolution TEM of SiC nanopillars, and Raman spectra of SiC nanofilms. Finally, we explain the kinetic mechanism of the WZ polytype formation in the ZB nanofilm based on the Si/C surface saturation control.

References

[1] Kojima K, Okumura H, Kuroda S and Arai K 2004 *J. Crystal Growth* **269** 367
[2] Liu K X, Stahlbush R E, Lew K K, Myers-Ward R L, Vanmil B L, Gaskill K D and Eddy C R 2008 *J. Electron. Mater.* **37** 730

[3] Sun G S, Liu X F, Wu H L, Yan G G, Dong L, Zheng L, Zhao W S, Wang L, Zeng Y P, Li X G and Wang Z G 2011 *Chin. Phys. B* **20** 033301
[4] Sun J W, Ivanov I G, Liljedahl R, Yakimova R and Syvajarvi M 2012 *Appl. Phys. Lett.* **100** 252101
[5] Saito E, Filimonov S and Suemitsu M 2010 *Mater. Sci. Forum.* **645–648** 147
[6] Das H, Melnychuk G and Koshka Y 2010 *J. Crystal Growth* **312** 1912
[7] Kotamraju S, Krishnan B, Melnychuk G and Koshka Y 2010 *J. Crystal Growth* **312** 645
[8] Kim B, Coy J, Kim S and Capano M 2009 *J. Electron. Mater.* **38** 581
[9] Teker K, Jacob C, Chung J and Hong M H 2000 *Thin Solid Films* **371** 53
[10] Steckl A J, Yuan C, Li J P and Loboda M J 1993 *Appl. Phys. Lett.* **63** 3347
[11] Cloitre T, Moreaud N, Vicente P, Sadowski M L and Aulombard R L 2001 *Mater. Sci. Forum.* **353–356** 159
[12] Li W, Dimitrijev S, Jisheng H, Iacopi A, Hold L, Tanner P and Harrison H B 2011 *Thin Solid Films* **519** 6443
[13] Liu X F, Sun G S, Zhao Y M, Ning J, Li J Y, Wang L, Zhao W S, Luo M C and Li J M 2007 *Mater. Sci. Forum* **556–557** 109
[14] Hassan J, Bergman J P, Henry A and Janzen E 2008 *J. Crystal Growth* **310** 4424
[15] Hori T, Danno K and Kimoto T 2007 *J. Crystal Growth* **306** 297
[16] Leone S, Pedersen H, Henry A, Kordina O and Janzen E 2009 *J. Crystal Growth* **312** 24
[17] Li J, Batoni P and Tsu R 2010 *Thin Solid Films* **518** 1658
[18] Habermehl S, Rodriguez M and Simmons B 2012 *J. Appl. Phys.* **112** 013535
[19] Sun G S, Liu X F, Wang L, Zhao W S, Yang T, Wu H L, Yan G G, Zhao Y M, Ning J, Zeng Y P and Li J M 2010 *Chin. Phys. B* **19** 088101
[20] Zhao Y M, Sun G S, Ning J, Liu X F, Zhao W S, Wang L and Li J M 2008 *Chin. Phys. Lett.* **25** 2269
[21] Joyce H J, Wong-Leung J, Gao Q, Tan H H and Jagadish C 2010 *Nano Lett.* **10** 908
[22] Verheijen M A, Algra R E, Borgstrom M T, Immink G, Sourty E, van Enckevort W J P, Vlieg E and Bakkers E P A M 2007 *Nano Lett.* **7** 3051
[23] Intarasiri S, Hallen A, Lu J, Jensen J, Yu L D, Bertilsson K, Wolborski M, Singkarat S and Possnert G 2007 *Appl. Surf. Sci.* **253** 4836
[24] Zhang X, Li L, Skowronski M, Sumakeris J J, Paisley M J and O'Loughlin M J 2009 *J. Appl. Phys.* **105** 123529
[25] Nishimura T, Satoh M, Jinushi T, Saitou Y and Nakamura T 2012 *Nucl. Instrum. Methods Phys. Res. Sect. B: Beam Interact. Mater. Atoms* **272** 422
[26] Lebedev A A 2006 *Semicond. Sci. Technol.* **21** R17
[27] Nakashima S and Harima H 1997 *Phys. Status Solidi A: Appl. Res.* **162** 39
[28] Temple P A and Hathaway C E 1973 *Phys. Rev. B* **7** 3685
[29] Rohmfeld S, Hundhausen M, Ley L, Zorman C A and Mehregany M 2002 *J. Appl. Phys.* **91** 1113
[30] Perova T S, Wasyluk J, Kukushkin S A, Osipov A V, Feoktistov N A and Grudinkin S A 2010 *Nanoscale Res. Lett.* **5** 1507
[31] Fissel A 2003 *Phys. Rep.* **379** 149